Flux expulsion by a point vortex

K. BAJER

ABSTRACT. – The Batchelor-Prandtl theory of high-Reynolds-number steady two-dimensional flows predicts uniform vorticity in regions of closed streamlines. The same argument applies to the gradients of a passive tracer and to the magnetic field in a conducting fluid which are also expelled from the eddies. In this case the problem is linear and allows more detailed analysis of the homogeneization process which turns out to be much faster than diffusion.

Here we consider the expulsion of the magnetic flux. A vertical line vortex is 'switched on' in a horizontal magnetic field. When boundaries are present we find a simple analytical solution for the steady state. In an infinite domain we find a family of similarity solutions with the field lines forming a spiral structure propagating away from the vortex. The similarity solution approximates the evolution well in the bounded domain and explains the scaling laws of various physical quantities at intermediate times when the expulsion process is in progress.

This model of flux expulsion is relevant when the magnetic Prandtl number is large, so that the line vortex spreads much more slowly than the 'hole' in the field created around it. The problem when the horizontal field suffering expulsion is vorticity rather than a magnetic field was recently considered by Kawahara *et al.* (1996). © Elsevier, Paris

1. Introduction

If a weak magnetic field penetrates a conducting fluid in two-dimensional motion then its components in the plane of the flow are expelled from the regions of recirculating flows with closed streamlines, such as isolated strong eddies or convective rolls. This process has influence on the morphology of the field shaping it in the form of tubes, ropes or sheets near the border regions between eddies. When this happens the evolution and properties of the field are best described in terms of such individual flux structures. For astrophysical fields, especially in and above the solar convection zone this fruitful approach is often adopted, so it is important to understand the underlying process by which the field is concentrated and fragmented. In the core of the recirculating region the component of the field remains aligned with the vorticity. The structure of such a vortex has been analysed by Bajer (1995), Bajer and Moffatt (1997). In the present paper we focus on the process of expulsion.

The principle of the expulsion mechanism is the continuous decrease of the characteristic length-scale of the advected quantity whose growing gradients cause accelerated diffusion. The gradients of vorticity in a bounded two-dimensional flow with high Reynolds number are eliminated in such a way leaving, according to the Batchelor-Prandtl theorem, a steady flow in which the vorticity is uniform (Batchelor, 1956). The theorem is concerned with the final steady state, but does not explain the details of the homogeneization process.

These were later considered by Weiss (1966) who analysed the related problem of the expulsion of the horizontal magnetic field from isolated strong eddies and from arrays of convective rolls with prescribed velocity field. Here the quantity whose gradients are expelled is the flux function. When the field is weak the associated Lorenz force has little effect on the flow, so the kinematic approach is justified; that is the magnetic field is passive and the velocity field can be regarded as given, which makes the expulsion problem linear. This is a considerable simplification compared with Batchelor's problem of the homogeneization of vorticity, which is not a passive quantity, and there is no such thing as an independently given background flow. In his numerical simulations Weiss found initial amplification of the magnetic energy up to $B_0^2 R_m^{2/3}$ where R_m is the magnetic Reynolds number and B_0 is the magnitude of the initial field. When the flux expulsion was completed

University of Warsaw, Institute of Geophysics, ul. Pasteura 7, 02-093 Warsaw, Poland. www.ifg.fuw.edu.pl/~kb/WWW

the energy dropped to $B_0^2 R_m^{1/2}$. The time-scale of the process appeared to be $t_0 R_m^{1/3}$, intermediate between the turnover time t_0 and the diffusive time-scale $t_d = t_0 R_m$.

Moffatt and Kamkar (1983) solved a simple model with periodic magnetic field in the uniform shear flow exactly. They also did an intermediate-time asymptotic analysis for the initially uniform field in arbitrary axisymmetric flows. In both cases they derived the $t_0 R_m^{1/3}$ time-scale.

Rhines and Young (1983) have considered the formally equivalent problem of the homogeneization of the passive scalar within closed streamlines. The scalar corresponds to the flux function, its gradients to the magnetic field and the Peclet number Pe is the counterpart of R_m. Rhines and Young have pointed out that the expulsion process does not eliminate *all* gradients. If the Fourier decomposition of the initial distribution of the scalar contains an axisymmetric mode $\theta_0(r)$, then it will evolve on its own time-scale, possibly $t_0 Pe$, determined by the initial radial gradients of θ_0 while all the non-axisymmetric modes $\theta_n(r) e^{in\theta}$ will be expelled by the time $t \sim t_0 Pe^{1/3}$. Hence the expulsion process may leave an axisymmetric distribution with radial gradients diffusing at the normal rate. This was verified numerically by Bernoff and Lingevitch (1994).

Recently Kawahara *et al.* presented a large-Reynolds number asymptotic theory of the interaction between a straight vortex tube inclined at an angle to the vorticity of the simple shear flow. This is a complex non-linear process. but the expulsion of the component of the background vorticity normal to the tube is the key ingredient. Due to nonlinearity the spirals of the normal vorticity stretch the axial vorticity. The combination of these two effects may help to explain the observed tendency of two interacting vortex tubes to turn antiparallel just before the onset of reconnection. Both the strong vorticity in the tube and that of the background flow diffuse at the same rate and such lack of the separation of scales adds extra complication in their case. For this reason no time dependent solutions were found that could be expressed in terms of known special functions and there is no steady state for any realistic boundary condition.

In the present paper we consider the expulsion of the initially uniform magnetic field by the localised axisymmetric vortex. We look at a length-scale much larger than the size of the eddy. At this scale the flow is that of a point vortex. In section 2 we assume the presence of the circular perfectly conducting solid boundary surrounding the cylindrical cavity filled with fluid. with the vortex on its axis. We find a simple exact expression for the steady state with the field lines expelled from the interior of the cavity and forming a double logarithmic spiral concentrated in a thin boundary layer near the solid surface.

In section 3 we consider an unbounded domain and find a self-similar solution showing flux expulsion. The solution can be written in terms of a known special function which can be computed from its integral representation. The self-similar solution yields the scaling laws for various quantities, for example the expected intermediate time-scale of the expulsion process. Some of the scaling laws are different in the self-similar solution and in the bounded domain.

In section 4 we give a short qualitative description of the time-dependent problem in the cylindrical cavity which explains the scaling of the peak magnetic energy (Weiss, 1966) assuming the self-similar nature of the transient. Finally, in section 5 we discuss the results.

2. Steady state in a cylindrical cavity in a perfect conductor

We consider a perfectly conducting solid with a vertical cylindrical cavity $0 \leq r \leq R$ filled with fluid having magnetic diffusivity η. We assume the flow to be incompressible and axisymmetric so that in polar coordinates (r, θ) velocity is given by the stream function $\Psi(r)$,

$$\text{(1)} \qquad \mathbf{u} = -\frac{d\Psi}{dr} \hat{\mathbf{e}}_\theta.$$

Any such flow satisfies the Euler equation, so in a viscous fluid it will evolve on a diffusive time-scale unless it is unstable.

Both the solid and the fluid are penetrated by the magnetic field $\mathbf{B}\,(r.\ \theta)$ given by its flux function $A\,(r.\ \theta)$

(2)
$$\mathbf{B} = (B_r,\ B_\theta,\ 0) = \left(\frac{1}{r}\frac{\partial A}{\partial \theta},\ \frac{\partial A}{\partial r},\ 0\right),$$

which evolves according to the induction equation:

(3)
$$\frac{\partial A}{\partial t} = \frac{1}{r}\frac{d\Psi}{dr}\frac{\partial A}{\partial \theta} + \eta\nabla^2 A.$$

At the initial instant $t = 0$ the field is uniform, see Figure 1, and in the (perfectly conducting) solid it remains uniform for all time, so the flux function satisfies

(4)
$$A\,(r = R,\ \theta,\ t) = B_0 R \sin\theta.$$

(5)
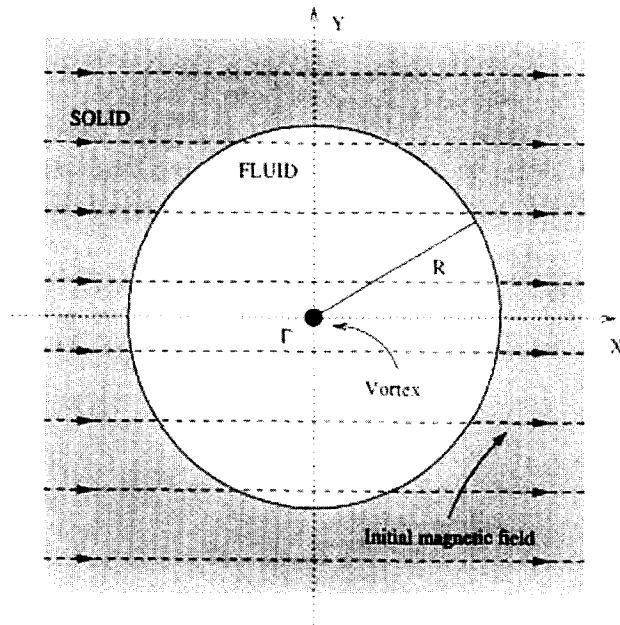$$A\,(r,\ \theta.\ t = 0) = B_0 r \sin\theta.$$

Fig. 1. – Solid with fluid-filled cylindrical cavity penetrated by the magnetic field which is uniform at $t = 0$.

In an axisymmetric flow the Fourier modes of A evolve independently and only one of them is present at $t = 0$, so the solution takes the form

(6)
$$A\,(r.\ \theta.\ t) = \mathrm{Re}\,[f\,(r,\ t)\,e^{i\theta}].$$

Choosing dimensionless variables,

(7)
$$r = Rr^*;\qquad t = \frac{R^2}{\eta}t^*;\qquad f = B_0 R f^*;\qquad \Psi = \frac{\Gamma}{2\pi}\Psi^*.$$

where Γ is the total circulation in the cavity, we obtain (dropping *) the following equation for the radial part of the flux function:

$$(8) \qquad \frac{\partial f}{\partial t} = f'' + \frac{1}{r} f' + \left(\frac{\mathrm{i} R_m}{r} \frac{d\Psi}{dr} - \frac{1}{r^2} \right) f,$$

$$(9) \qquad f\,(r = 1,\, t) = -\mathrm{i}, \qquad f\,(r,\, t = 0) = -\mathrm{i} r,$$

where $'$ denotes d/dr and

$$(10) \qquad R_m = \frac{\Gamma}{2\pi \eta}$$

is the magnetic Reynolds number. The axisymmetric flow will rapidly wrap the initially uniform field into a spiral.

Let us consider a special case when the flow is due to a point vortex, *i.e.*

$$(11) \qquad \Psi = -\ln r.$$

Equation (8) then takes the following form:

$$(12) \qquad \frac{\partial f}{\partial t} = f'' + \frac{1}{r} f' - \left(\frac{1 + \mathrm{i} R_m}{r^2} \right) f.$$

The details of the evolution are rather complex and the solution of the initial value problem (12) must be obtained numerically, however the final steady state takes a particularly simple form:

$$(13) \qquad f\,(r) = -\mathrm{i} r^\alpha, \qquad \text{where} \quad \alpha = (1 + \mathrm{i} R_m)^{1/2}.$$

In Figure 2 we show the field lines of this solution for $R_m = 1,\ 10,\ 100$ and 500. When $R_m \gg 1$ we have

$$(14) \qquad f\,(r,\, \theta) \approx -\mathrm{i} r^{\left(\frac{1}{2} R_m \right)^{1/2} (1 + \mathrm{i})}$$

$$(15) \qquad A\,(r,\, \theta) \approx r^{\left(\frac{1}{2} R_m \right)^{1/2}} \sin \left[\left(\frac{1}{2} R_m \right)^{1/2} \ln r + \theta \right]$$

$$(16) \qquad B_r(r,\, \theta) \approx r^{\left(\frac{1}{2} R_m \right)^{1/2} - 1} \cos \left[\left(\frac{1}{2} R_m \right)^{1/2} \ln r + \theta \right]$$

$$(17) \qquad B_\theta(r,\, \theta) \approx -R_m^{1/2} r^{\left(\frac{1}{2} R_m \right)^{1/2} - 1} \cos \left[\left(\frac{1}{2} R_m \right)^{1/2} \ln r + \theta - \frac{1}{4} \pi \right],$$

so the field lines form a (double) logarithmic spiral. The energy stored in the radial and angular components of the magnetic field is

$$(18) \qquad \left\langle \frac{1}{2} B_r^2 \right\rangle = \frac{1}{4} \sqrt{2\pi}\, R_m^{-1/2} \qquad \text{and} \qquad \left\langle \frac{1}{2} B_\theta^2 \right\rangle = \frac{1}{4} \sqrt{2\pi}\, R_m^{1/2}$$
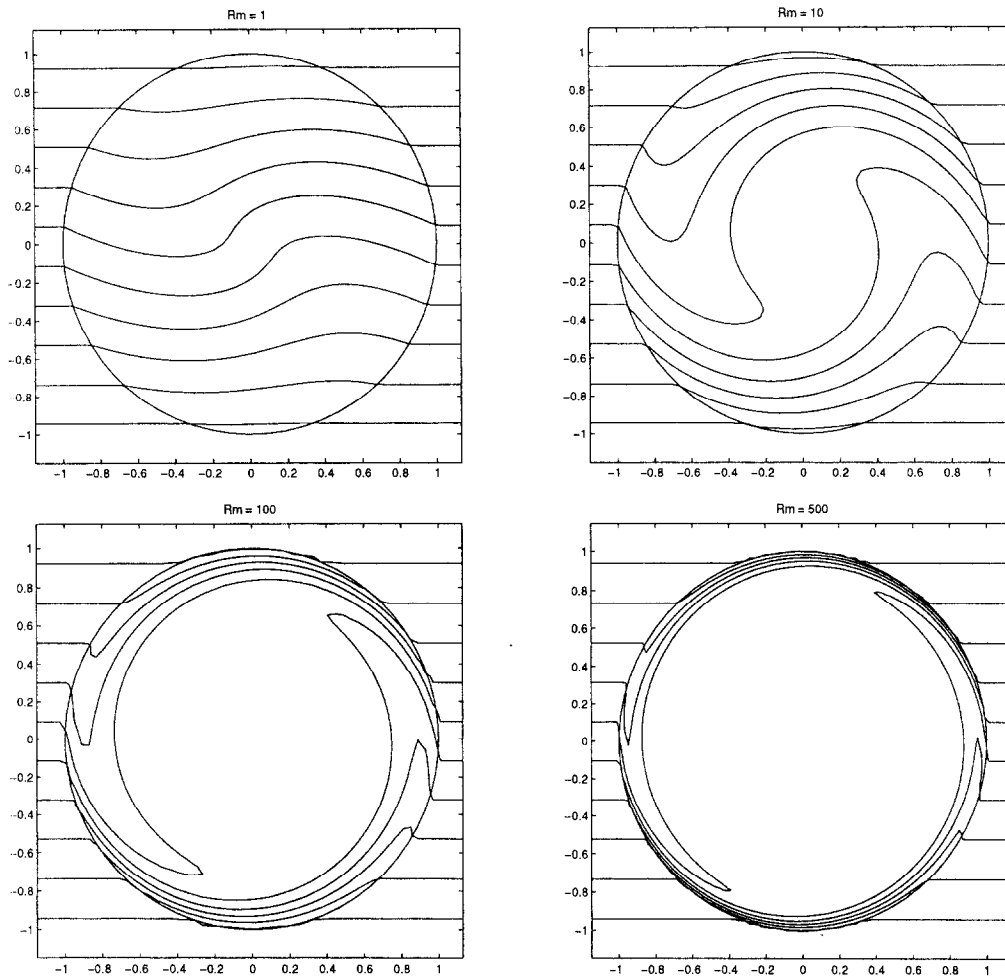
Fig. 2. – The field lines of the steady-state solution (13) with different values of R_m.

where $\langle\ \rangle$ denotes integration over the cavity, so the radial component is virtually eliminated while the angular component is greatly enhanced.

Figure 2 clearly shows that for large R_m, as expected, a magnetic boundary layer forms near the solid surface. Let us define the width δ of such layer to be the distance from the wall where B_θ drops to $\mathrm{e}^{-4} \approx 2\%$ of its value on the boundary. We obtain:

$$(19) \qquad \delta = 1 - \exp\left[\frac{-4}{\left(\frac{1}{2}R_m^{1/2}\right)-1}\right] = 4\left(\frac{1}{2}R_m\right)^{-1/2} + O(R_m^{-1}) \qquad \text{when} \quad R_m \gg 1.$$

This scaling is often encountered in high-R_m computational magnetohydrodynamics, but here we obtain it rigorously from an analytically given steady state. As we move inwards the field changes sign at

$$(20) \qquad r_n = \exp\left[-n\,\pi\left(\frac{1}{2}R_m\right)^{-1/2}\right].$$

so $(1 - r_m)/\delta \approx \frac{\pi}{4} n$ and it is clear that the bondary layer contains only one turn of the spiral. Another length of interest is the distance δ_B from the wall where the field strength drops below its value in the surrounding solid:

$$(21) \qquad \delta_B = 2^{-1/2} R_m^{-1/2} \ln R_m + O\left(R_m^{-1}\right),$$

so that $\delta_B/\delta = \frac{1}{8} \ln R_m + O\left(R_m^{-1/2}\right)$. At any fixed radius the magnitude of the field goes to zero as $R_m \to \infty$, so the vortex really creates a 'hole' in the field, but when $R_m \gg 10^4$ the field is enhanced, as compared to its magnitude in the surrounding solid, even outside the boundary layer.

The magnetic boundary layer is the region of large energy dissipation. The electric current is vertical, $\mathbf{j} = j\,(r,\,\theta)\,\hat{\mathbf{e}}_z$, and equals

$$(22) \qquad j\,(r,\,\theta) = -R_m r^{j-2} \left[\cos\left(\beta \ln r + \theta\right) - R_m^{-1} \sin\left(\beta \ln r + \theta\right)\right]$$

where $\beta = \left(\frac{1}{2} R_m\right)^{1/2}$. This is the source of Ohmic heating of the fluid filling the cavity with the total rate of

$$(23) \qquad \Phi_m = R_m^{-1} \int_0^{2\pi} d\theta \int_0^1 dr\, j^2 = 2^{-1/2}\, \pi R_m^{1/2} + O\left(R_m^{-3/2}\right).$$

Hence, the current-sheet in the boundary layer dissipates the magnetic energy very efficiently, at a rate increasing with R_m. This is in contrast to the situation in the Burgers-layer-type current sheet forming when two magnetic flux elements are pushed against each other by a straining flow. Then a current sheet also forms, i.e., the current increases with R_m, but the total rate of dissipation *decreases* as $R_m^{-1/2}$. This is an important issue in solar physics where it is still not entirely clear whether current sheets in the solar corona are the sources of direct heating or whether they only break the topological constraints, enabling further relaxation.

3. Unbounded domain

Let us now assume that the fluid fills the entire space rather than cylindrical cavity. Again a point vortex is switched on at the initial instant $t = 0$ and starts distorting the initial field which, in this case, does not have to be uniform. There is no natural length-scale in the problem, so we expect a self-similar solution to exist, depending on the usual similarity variable $\frac{1}{4} r^2/t$. The following change of variables,

$$(24) \qquad w = \frac{r^2}{4t}, \qquad \tau = \ln t, \qquad H = t^{-p} w^{-\alpha} \mathrm{e}^w f,$$

where p is an arbitrary (real) constant, gives an equation for H:

$$(25) \qquad \frac{\partial H}{\partial \tau} = w H'' + (2\alpha + 1 - w)\,H' - (\alpha + 1 + p)\,H.$$

Up to a constant factor there is one steady-state solution regular at the origin,

$$(26) \qquad H\,(w) = -2\mathrm{i}\,\frac{\Gamma\,(\alpha + 1 + p)}{\Gamma\,(2\alpha + 1)}\, M\,(\alpha + 1 + p,\ 2\alpha + 1;\ w),$$

where $M = {}_1F_1$ is the confluent hypergeometric function also called Kummer's function (Abramowitz and Stegun, 1970, § 13.1). In the original variables we obtain

$$(27) \qquad f\,(r,\,t) = -2\mathrm{i}\,\frac{\Gamma\,(\alpha + 1 + p)}{\Gamma\,(2\alpha + 1)}\, t^p \left(\frac{r^2}{4t}\right)^\alpha \mathrm{e}^{-r^2/4t}\, M\left(\alpha + 1 + p,\ 2\alpha + 1,\ \frac{r^2}{4t}\right).$$

This one-parameter family of similarity solutions labeled by p has the following asymptotic behaviour:

$$(28) \qquad f \sim -2\mathrm{i} \left(\frac{r^2}{4}\right)^p, \qquad r \to \infty, \qquad t \text{ fixed.}$$

When $p = \pm\frac{1}{2}$ the field at large distances is current-free, so it is in magnetostatic equilibrium and the vortex makes a hole in it when it is switched on. With $p = \frac{1}{2}$ the far field is uniform and with $p = -\frac{1}{2}$ it is the field of the dipolar current. Other solutions with $p < \frac{1}{2}$ have finite magnetic energy, so they are also physicaly meaningful. They correspond to dipolar current distributions with current decreasing algebraically with r. Unlike equilibria with $p = \pm\frac{1}{2}$ these current distributions with algebraic tails could not exist without the central vortex. If left to itself the field at large distances would decay and vanish. However, due to the central vortex, current at any given distance would be maintained for some time until the void in the field reaches that distance.

Let us now consider the case of the uniform far field, $p = \frac{1}{2}$, in greater detail. When the vortex is switched on, the similarity solution (27) is *immediately* established. This is because, quite remarkaly, it satisfies not only equation (12), but also the initial uniform field condition, $f(r, t = 0) = -\mathrm{i}r$ (Abramowitz and Stegun, 1970, § 13.5.1). Such a coincidence is possible because the initial field, like the point vortex flow, does not have any natural length-scale.

The function M in (27) is defined as an infinite series in the usual way, but the numerical summation of this series becomes impractical as the number of terms needed is proportional to R_m. The following integral representation of M is easier to handle:

$$(29) \qquad \frac{\Gamma(\alpha + 3/2)}{\Gamma(2\alpha + 1)} \mathrm{e}^{-w} M(\alpha + 3/2, 2\alpha + 1, w) = \int_0^1 \mathrm{e}^{-wt} (1 - t)^{\alpha + 1/2} t^{\alpha - 3/2} \, dt,$$

which gives

$$(30) \qquad B_\theta(r, \theta = \pi/2, t) = \mathrm{Im}\left(\frac{\partial f(r, t)}{\partial r}\right)$$

$$= \mathrm{Im}\left\{ ew\beta^{-1/2} \int_0^1 \mathrm{e}^{-wt} \left(\beta + \frac{1}{2} - wt\right) (1 - t)^2 \left[\frac{ew(1 - t)t}{\beta}\right]^{\beta - 1} dt \right\}.$$

The terms in the integral are arranged in such way as to minimise the absolute value of the numbers obtained at intermediate steps of the computation. In Figure 3 we plot the profile of the angular component of the magnetic field versus $rt^{-1/2}$ for $R_m = 10^1$, 10^2, 10^3 and 10^4.

Further increase of R_m is limited by the machine precision, effects of which we can already notice at $R_m = 10^4$ when $rt^{-1/2} > 75$. The expulsion of the magnetic flux shows quite clearly. In a rather sharply outlined region around the point vortex the field vanishes. Further out the field is greatly enhanced where several turns of the spiral pile up and then decrease down to $B_\theta = 1$ of the uniform background. As time increases the entire structure moves outward.

Let us now consider the scaling of different quantities with magnetic Reynolds number. From Figure 3 we can easily find the peak value of B_θ which is of the order

$$(31) \qquad \frac{B_p}{B_0} = O(R_m^{1/3}).$$

In order to find the scaling of the radius r_h of the central hole in the field, in Figure 4 we superimpose plots of $-B_\theta^{-1/3}$ versus $rt^{-1/2}R_m^{-1/3}$ for $R_m = 10^3$ and 10^4.
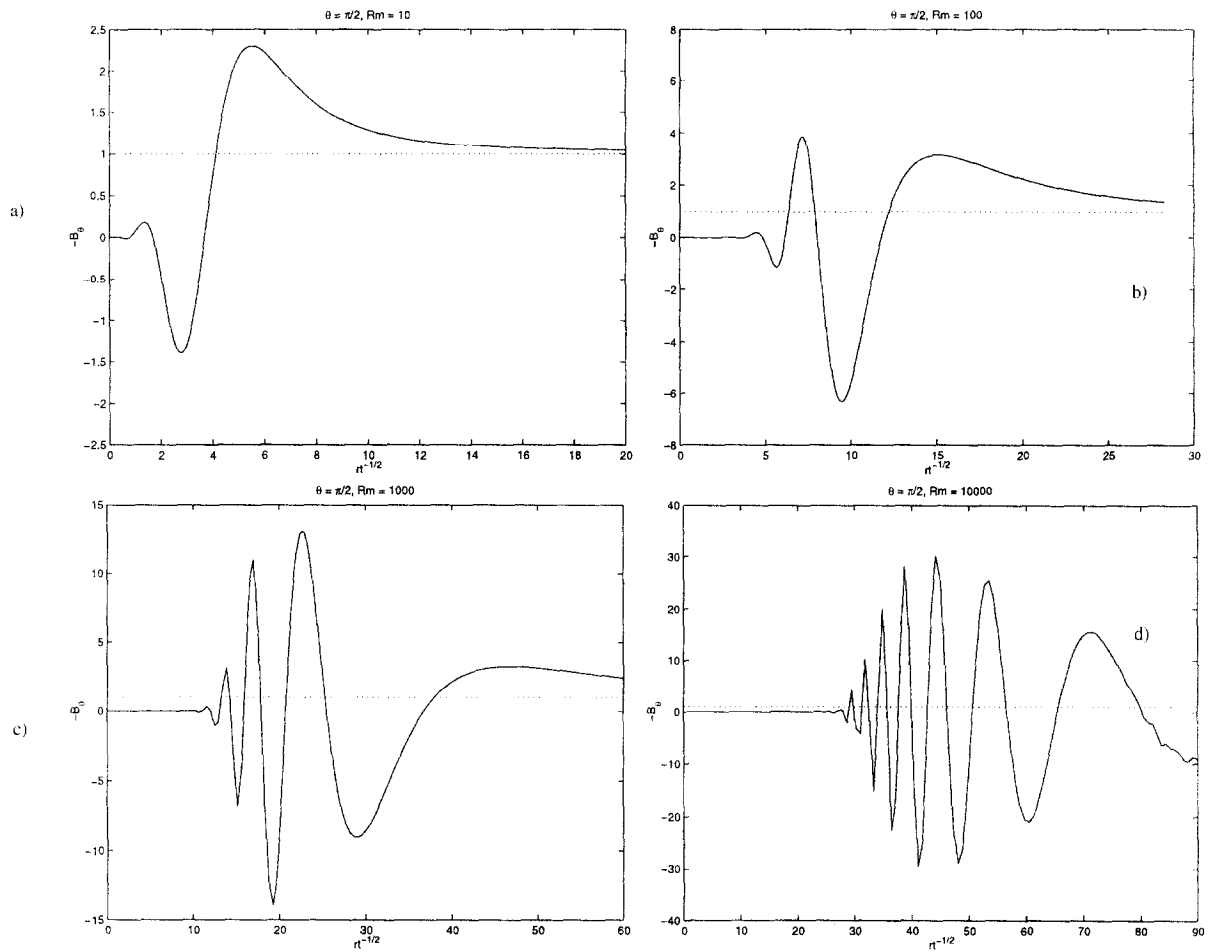
Fig. 3. – The component $-B_\theta$ at $\theta = \pi/2$ versus $rt^{-1/2}$ for the self-similar solution (27) with:
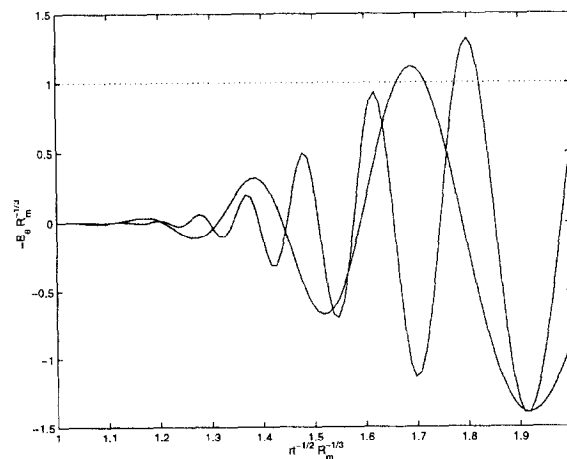a) $R_m = 10$; b) $R_m = 100$; c) $R_m = 1000$ and d) $R_m = 10000$.

Fig. 4. – The plots of $B_\theta R_m^{-1/3}$ versus $rt^{-1/2}R_m^{-1/3}$ for $R_m = 10^3$ and $R_m = 10^4$. With such scaling the envelopes of the two solutions coincide which shows that the size of the 'hole' in the field scales with $R_m^{1/3}$.

The envelopes of the two solutions coincide which means that in the *dimensionless* units we have:

$$(32) \qquad \frac{r_h}{R} \sim \left(\frac{t}{t_d R_m^{-2/3}} \right)^{1/2}$$

where t_d is the diffusive time-scale associated with the length-scale R (see eq. 7). In the case of the similarity solution there is no natural length-scale, so R is arbitrary.

Hence the radius of the outer edge of the hole in the field (the tail of the 'wawepacket') increases as $t^{1/2}$ and the time-scale of this flux expulsion process is

$$(33) \qquad t_{fe} = t_d R_m^{-2/3}.$$

This time-scale, fast compared to t_d yet slower than the advective time-scale t_{adv}, was found in the computations of Weiss (1966) and was later given theoretical support by Moffatt and Kamkar (1983), who considered a simple shear flow and explained how it reduces the length-scale, thus leading to such an accelerated diffusion. This intermediate time-scale was also found in a related problem of the homogeneization of a passive scalar by expulsion of its gradients (Rhines and Young, 1983).

Somewhat less clear is the scaling of the radial extent Δr of the region D_f where the field is significantly increased above its value at large distances. Reading the position of the last maximum in Figure 3 we can make an estimate:

$$(34) \qquad \frac{\Delta r}{R} \sim \left(\frac{t}{t_d R_m^{-1}} \right)^{1/2}.$$

Hence, the characteristic time-scale on which the region D_f is spreading is

$$(35) \qquad t_{adv} = t_d R_m^{-1}$$

that is the *advective* time-scale associated with length R. The front of the region of the enhanced field is moving faster than its tail and this determines the growth of the surface area of D_f,

$$(36) \qquad \frac{S}{R^2} \sim \frac{t}{t_d R_m^{-1}}$$

and the total magnetic energy

$$(37) \qquad \frac{E_m}{R^2 B_0^2} \sim \frac{S}{R^2} \frac{B_p^2}{B_0^2} \sim \frac{t}{t_d R_m^{-5/3}}.$$

The number N of oscillations of B_θ in the region D_f grows as $R_m^{1/3}$, so the characteristic length-scale of the field is:

$$(38) \qquad \frac{l}{R} \sim \frac{\Delta r}{RN} \sim \left(\frac{t}{t_d R_m^{-1/3}} \right)^{1/2}$$

and the electric current

$$(39) \qquad \frac{j}{B_0/R} \sim \frac{B_p}{B_0} \left(\frac{l}{R} \right)^{-1} \sim \left(\frac{t}{t_d R_m^{1/3}} \right)^{-1/2}.$$

Asymptotically the total ohmic dissipation is independent of time and equals:

$$(40) \qquad \Phi_m \sim R_m^{-1} \frac{S}{R^2} \left(\frac{j}{B_0/R} \right)^2 \sim R_m^{1/3}.$$

In Table I we summarize all these scaling laws for the steady state in a cylindrical cavity and for the self-similar solution at fixed dimensionless time τ. The scaling of the latter depends on the choice of the unit of time. Both the scaling on the diffusive and the advective time-scale are shown.

TABLE I. – Scaling of various (dimensionless) quantities in the steady state inside a cylindrical cavity and in the self-similar solution at fixed time τ. The scalling laws depend on whether time is fixed on the diffusive time-scale (third column) or the advective time-scale (fourth column). r_h – radius of the 'hole' in the field; B_p – preak field; Δr – radial extent of the region D_f where the field is significant; N – number of field peaks in D_f; l – characteristic length-scale of the field; j – current; S – surface area of D_f; E_m – total magnetic energy; Φ_m – total ohmic dissipation.

	Cylindrical cavity	Self-similar solution $\tau = t/t_d$	Self-similar solution $\tau = t/t_{adv}$
r_h	1	$\tau^{1/2} R_m^{1/3}$	$\tau^{1/2} R_m^{-1/6}$
B_p	$R_m^{1/2}$	$R_m^{1/3}$	$R_m^{1/3}$
B_p^2	R_m	$R_m^{2/3}$	$R_m^{2/3}$
Δr	$R_m^{-1/2}$	$\tau^{1/2} R_m^{1/2}$	$\tau^{1/2}$
N	1	$R_m^{1/3}$	$R_m^{1/3}$
l	$R_m^{-1/2}$	$\tau^{1/2} R_m^{1/6}$	$\tau^{1/2} R_m^{-1/3}$
j	R_m	$\tau^{-1/2} R_m^{1/6}$	$\tau^{-1/2} R_m^{2/3}$
S	$R_m^{-1/2}$	τR_m	τ
E_m	$R_m^{1/2}$	$\tau R_m^{5/3}$	$\tau R_m^{2/3}$
Φ_m	$R_m^{1/2}$	$R_m^{1/3}$	$R_m^{1/3}$

4. Time-dependent problem in the cylindrical cavity

Let us now revert to the problem of the earlier section with a point vortex at the center of the cylindrical cavity whose radius now imposes a natural length-scale R.

With the help of the scaling laws we can now formulate a qualitative description of the time-dependent expulsion process. After the vortex is switched on at $t = 0$ we expect the similarity solution (27) to be established. In the limit $t \to 0$ this solution satisfies the initial condition (uniform field) everywhere except at the origin where the field vanishes. As in many other diffusive problems, at the initial instant there is probably a sudden jump of the field value at $r = 0$ and the self-similar solution is established *instantaneously*.

This solution is valid when $t \lesssim t_{adv}$, that is until the front of the perturbation (region D_f) arrives at the solid boundary which happens when $\Delta r/R \sim 1$ (see Table I). During this phase the total magnetic energy grows linearly with time, $E_m \sim \tau R_m^{2/3}$, reaching a peak value proportional to $R_m^{2/3}$. This is precisely the behaviour found in the numerical simulations by Weiss (1966) who used a regular flow field with a single

eddy imitating a convective roll. This means that the scaling we found applies to a broad class of flows and is not specific to the point vortex.

At time $t \sim t_{adv}$ the transition begins from the similarity solution (27) to the steady state (13). The radius of the hole in the field is then $r_h \sim R_m^{-1/6}$ and keeps growing until $t \sim t_{adv}^{1/3}$ when $r_h \sim 1$, the flux expulsion is completed and the field reaches the steady state (13). Table I shows that E_m *drops* to $R_m^{1/2}$, also in agreement with the computational results (Weiss, 1966).

Another quantity of interest, especially in the astrophysical context, is the total ohmic dissipation which contributes to the heating of the fluid carrying the field, at the expense of the magnetic energy. During the self-similar phase the dissipation is constant in time and proportional to $R_m^{1/3}$. Then it *increases* to $R_m^{1/2}$ in the steady state.

5. Discussion

We have found a simple steady-state solution in a cylindrical cavity with perfectly conducting walls and a point vortex at the centre. In the real fluid with finite viscosity the central vortex will diffuse and a viscours boundary layer will grow from the wall inwards. However, as long as the Reynolds number Re is much larger than R_m our solution will describe a quasi-steady state lasting from times $t_{adv}R_m \ll t \ll t_{adv}$Re, provided the field is weak enough not to have any significant braking effect on the flow. This is truen when the Lorenz force is smaller than the inertial term,

$$(41) \qquad\qquad\qquad\qquad |\mathbf{j} \wedge \mathbf{B}| \lesssim |\mathbf{u} \cdot \nabla \mathbf{u}|.$$

In the boundary layer $|\mathbf{j} \wedge \mathbf{B}| \sim (B_0^2/R) R_m^{3/2}$ (see Table I), so the initial field must satisfy

$$(42) \qquad\qquad\qquad\qquad B_0^2 \lesssim (\Gamma/R)^2 R_m^{-3/2}$$

to justify the kinematic approach.

The time-dependent problem does not have as simple a solution as the steady state. However, for times shorter than the turnover time the solid boundary has little effect and the evolution of the uniform initial field is much the same as if it were in an unbounded domain. We found a self-similar solution describing this phase of the volution. Plotting the solution for different values of R_m we could estimate the scaling laws of various quantities of interest. In this exact solution the time-scale of the expulsion process is $t_{adv}R_m^{1/3}$, the same as in previous computations and asymptotic theories. The solution also explains the empirical scaling law (Weiss, 1966) for the peak magnetic energy $B_p^2 \sim B_0^2 R_m^{2/3}$. The total ohmic dissipation during the self-similar phase is independent of time and smaller than in the final steady state that follows.

Both the steady state and the similarity solution clearly show that the field is almost completely expelled from the central region. This is related to the special property of the initial condition (Rhines and Young, 1983). The flux function $A_0(r, \theta)$ of the uniform field has zero average over the streamlines of the flow (θ-average in this case). For the more general initial field the shear of the flow would average A_0 over θ expelling only its non-axisymmetric component. The reconnection would take place and closed circular field lines would appear around the vortex.

The time-dependent problem can, in principle, be solved exactly by the Laplace transform. This was done by Parker (1966) for the solid cylinder and sphere rotating in a vacuum. Due to the absence of shear the expulsion of flux happens on the diffusive rather than intermediate time-scale. In this special case the Laplace transform

can be inverted exactly, yielding a solution in the form of a series of orthogonal functions. This is not the case with the point vortex flow where the eigenvalue problem that needs to be solved is not self-adjoint.

The analysis presented in this paper can be applied directly to the expulsion of the gradients of a passive scalar, temperature for example. The evolution of the concentration of the scalar is governed by the same advection-diffusion equation (3) as the evolution of the flux function A. A concentrated vortex in the region of uniform temperature *gradients* will tend to homogenize temperature. In a cylindrical cavity with an initially uniform vertical gradient and fixed temperature of the solid wall the final state will be given by (13), f now meaning temperature and R_m the Peclet number, and the shape of the isotherms will be the same as in Figure 2. Similarly, the initial stage of the time-dependent problem is given by the solution (27).

REFERENCES

ABRAMOWITZ M., STEGUN I. A., 1970, *Handbook of Mathematical Functions*, Dover.

BAJER K., 1995, High Reynolds number vortices with magnetic field in non-axisymmetric strain. In *Small-Scale Structures in Three-Dimensional Hydrodynamic and Magnetohydrodynamic Turbulence* (ed. M. MENEGUZZI, A. POUQUET and P. L. SULEM), Lecture Notes in Physics, Springer., vol. **462**, 255-264.

BAJER K., MOFFATT H. K., 1977. On the effect of a central vortex on a stretched magnetic flux tube, *J. Fluid Mech.*, **339**, 121-142.

BATCHELOR G. K., 1956, On steady laminar flow with closed streamlines at large Reynolds number, *J. Fluid Mech.*, **1**, 177-190.

BERNOFF A. J., LINGEVITCH J. F., 1994, Rapid relaxation of an axisymmetric vortex, *Phys. Fluids*, **6**, 3717-3723.

KAWAHARA G., KIDA S., TANAKA M., YANASE S., 1996, Wrap, tilt and stretch of vorticity lines around a strong straight vortex tube in a simple shear flow, *J. Fluid Mech.*, **353**, 115-162.

MOFFATT H. K., KAMKAR H., 1983, The time-scale associated with flux expulsion. In *Stellar and Planetary Magnetism*, ed. A. M. SOWARD, Gordon and Breach.

PARKER R. L., 1966, Reconnection of lines of force in rotating spheres and cylinders, *Proc. Roy. Soc. A*, **291**, 60-72.

RHINES P. B., YOUNG W. R., 1983, How rapidly is a passive scalar mixed within closed streamlines, *J. Fluid Mech.*, **133**, 133-145.

WEISS N. O., 1966, The expulsion of magnetic flux by eddies, *Proc. Roy. Soc. A*, **293**, 310-328.